Mechanistic Tuning of Hydrocarbon Oxidations with H_2O_2, Catalyzed by Hexacoordinate Ferrous Complexes

Yasmina Mekmouche,[a] Stéphane Ménage,*[a] Jacques Pécaut,[b] Colette Lebrun,[b] Lee Reilly,[c] Volker Schuenemann,[c] Alfred Trautwein,[c] and Marc Fontecave[a]

Keywords: Iron catalysts / Hydrogen peroxide / Oxidation / Non-heme iron / Monooxygenase

A comparison of the catalytic properties of a series of $Fe^{II}LXY$ complexes on oxidation reactions with H_2O_2, [L = *N*,*N*′-bis(pyridin-2-yl-methyl)-*N*,*N*′-bis(3,4,5-trimethoxybenzyl)-ethane-1,2-diamine] indicates that the lability of the X and Y ligands (Cl^- or CH_3CN) determines the nature of the oxidation pathway. The absence of a labile site in the complex, i.e. when X = Y = Cl^-, causes the reaction to proceed via a Fenton pathway (generation of hydroxyl radicals, exclusively). The presence of two labile CH_3CN ligands (X = Y = CH_3CN) allows the catalysis to proceed through a metal-based mechanism, whereas in the case of a complex with only one labile ligand (X = Cl^- and Y = CH_3CN), the reaction is less controlled by the metal. We wish to emphasize that the cleavage of the O–O bond in the Fe–OOH moeity, a key intermediate in the reaction, is different in the last two cases.

Introduction

Synthetic non-heme ferrous complexes have been extensively studied due to their ability to mimic some structural and functional properties of non-heme iron monooxygenases or oxygen activating enzymes.[1] Some of the ligands used, mainly polydentate nitrogen-based, are shown in Scheme 1. These complexes have been found to be efficient catalysts for alkane oxidation using hydroperoxides or oxygen-donating reagents.[2] Few catalytic systems, however, allow selective oxidation of alkanes to the corresponding alcohol without formation of secondary products.[3] In the case of Fe and Mn porphyrins, such a selective reaction has been attributed to the involvement of a metal-oxo intermediate as the active species for the hydroxylation.[4] The question of the formation and the stabilization of such a species in non-heme systems has been the subject of extensive studies, and recently an Fe^{IV}=O system has been fully characterized.[5] Nevertheless, as soon as hydrogen peroxide is involved in the catalytic reaction as the oxidant, the nature of the reaction pathway is controversial. It usually alternates between a free radical (Fenton chemistry) or a metal based mechanism.[6] The identification of the essential stereoelectronic parameters, which control the reactivity of the active species, is still an important challenge. In particular, we demonstrated the importance of a labile site on the iron complex in order to allow the oxidant to bind, and to be activated.[7] Here, we will show from the reactivity pattern of a series of six-coordinate iron complexes $[Fe^{II}LXY](ClO_4)_n$ (L designating a tetradentate nitrogen based ligand and X, Y a monodentate ligand) that two labile sites are absolutely required for selective catalysis of alkane oxidation. The ligand L has been designed to serve as a substrate for probing the reaction mechanism. Indeed, L contains sites such as the methylene groups and the phenyl rings from benzylic moieties, which are vulnerable to oxidation. The latter are known to be very reactive towards hydroxyl radicals, leading to the formation of phenol.[8] Three hexacoordinate ferrous complexes, containing the tetradentate ligand L, [L = *N*,*N*′-bis(pyridin-2-yl-methyl)-*N*,*N*′-bis(3,4,5-trimethoxybenzyl)ethane-1,2-diamine],[8] the two remaining coordination sites being occupied either by a solvent molecule (known to be a labile ligand) or a chloride anion (known to be less exchangeable), have also been synthesized and fully characterized (Scheme 1).

The structure and catalytic properties of $FeLCl_2$ (**1**) and $FeL(CH_3CN)_2(ClO_4)_2$ (**2**) have been partly described previously.[9] In this paper they are compared, in more detail, with the structural, spectroscopic, and catalytic properties of a third new complex $FeLCl(CH_3CN)(ClO_4)$ (**3**), containing only one labile site. This complex completes the series.

[a] Laboratoire de Chimie et Biochimie des Centres Rédox Biologiques, Université Joseph Fourier/DRDC/CEA, UMR CNRS 5047,
17 rue des Martyrs, 38054 Grenoble Cédex 9, France
[b] Service de Chimie Inorganique et Biologique, DRFMC CEA-Grenoble, France
[c] Institut für Physik Medizinische Universität, Ratzeburger Allee 160, 23538 Lübeck, Germany
Supporting information for this article is available on the WWW under http://www.eurjic.org or from the author.

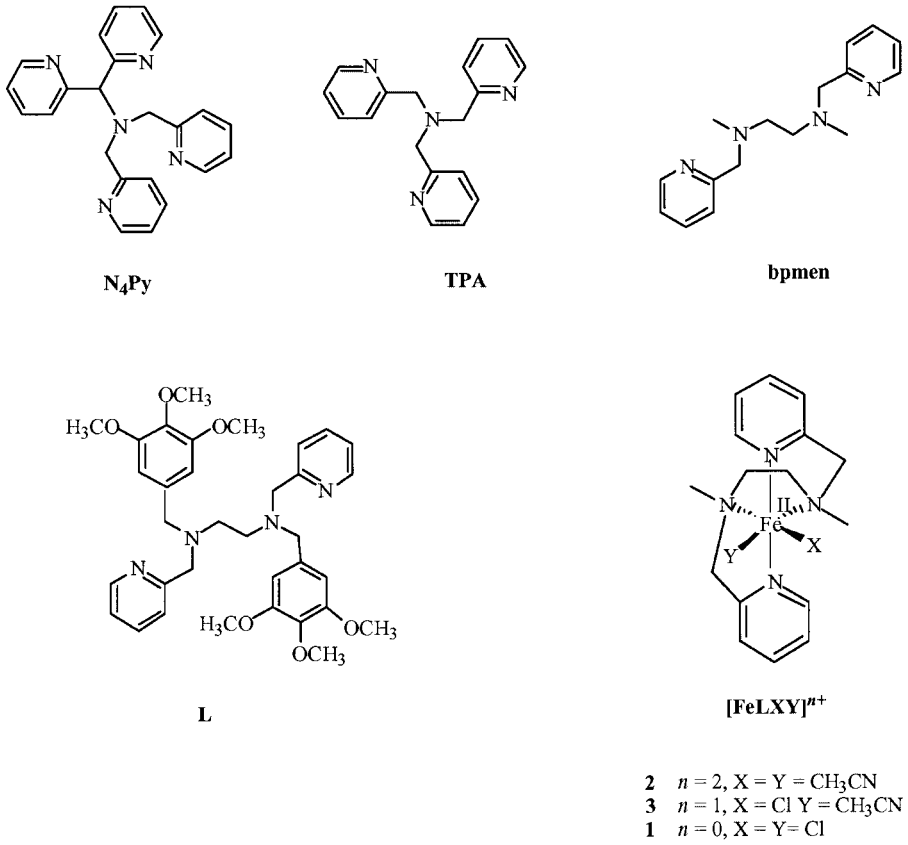

Scheme 1. Ligand used in this study, numbering scheme for the corresponding complexes, and related ligands discussed

Results

Syntheses of Complexes

The syntheses of complexes **1** and **2** are straightforward. Solid products were obtained by simply mixing equimolar amounts of ligand L and $FeCl_2{\cdot}4H_2O$ or $Fe(ClO_4)_2{\cdot}4H_2O$, respectively, in methanol under an inert atmosphere and at room temperature.[9] Complex **3** was synthesized via a two step procedure. When stoichiometric amounts of complexes **1** and **2** were mixed together in CH_2Cl_2 or $CHCl_3$ under argon, a light yellow microcrystalline powder was obtained. The reaction was quantitative, and the complex formed was identified, based on ESI/MS (see Exp. Sect.), as a dinuclear ferrous complex $[Fe_2L_2Cl_2](ClO_4)_2$. When the dinuclear complex was dissolved in acetonitrile it dissociated quantitatively into two identical $FeL(Cl)(CH_3CN)(ClO_4)$ units, i.e. complex **3**, which crystallizes in quantitative yield upon diffusion of ether into the mother liquor.

X-ray Structures of Complexes 1, 2, and 3

The structure of the cation present in the three complexes is represented in Figure 1. The Fe^{II} ion is in a pseudo-octahedral environment with the tetradentate ligand L wrapped around the metal ion. The two remaining coordination sites are filled by two chloride ions for **1**, two acetonitrile molecules for **2**, and one chloride and one acetonitrile for **3**. The topology consists of a *cis* α configuration for the monodentate ligands in each complex. Each one is *trans* with respect to one amine nitrogen atom and the pyridine ligands are *trans* to each other.

The Fe−ligand distances decrease as the number of CH_3CN ligands increases, reflecting the increase in ligand field strength in the following order: **1** < **3** < **2**. Accordingly, the shorter Fe−N distances (1.942−2.060 Å) are found in **2**, consistent with a low-spin configuration for its ferrous ion in the crystalline state, whereas the Fe−N distances (2.212−2.3272 Å) in **1** are longer than in **3** (2.1708−2.2787 Å), a range of distances is in agreement with a high-spin configuration for the ferrous ion in both complexes (see Table 1). Moreover, the $Fe-NCCH_3$ distance is longer in complex **3** [2.1730(8) Å] than in complex **2** [1.942(4) Å], and the Fe−Cl distance is shorter in complex **3** than in complex **1** [2.3383(3) compared with 2.4080(2)−2.4260(2) Å].

The presence of chloride anions is responsible for a distortion from the ideal octahedral geometry as shown by the more acute $N_{pyridine}-Fe-N_{pyridine}$ and $N_{amine}-Fe-N_{amine}$ angles in **1** and **3** compared with those in complex **2**. Accordingly, the presence of two Cl^- ions in a *cis* geometry leads to a larger X−Fe−Y angle [102.274(8) in **1** compared with 96.6(2) in the case of complex **3**].

The structural parameters of the $[Fe^{II}LXY]$ series are similar to those of the previously described $Fe(N_2Py_2)$ family represented, for example, by $[Fe(bpmen)(CH_3CN)_2]^{2+}$ or $(LBzl_2)FeCl_2$ [bpmen = *N*,*N*′-dimethyl-*N*,*N*′-bis(2-pyridyl-

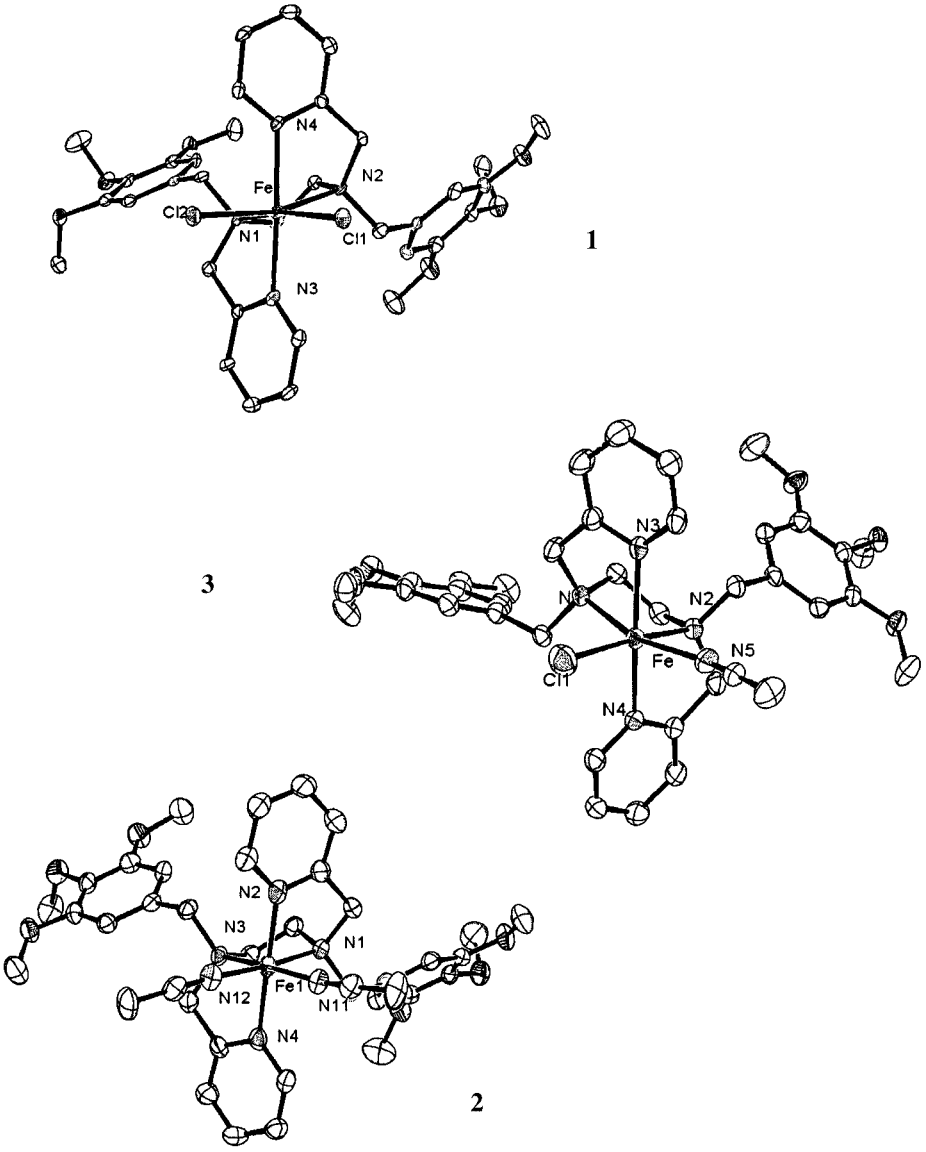

Figure 1. ORTEP representation of the cations of complexes **1**−**3**; all hydrogen atoms have been omitted for clarity

methyl)ethylene-1,2-diamine (Scheme 1), and $LBzl_2$ = *N*,*N*′-dibenzyl-*N*,*N*′-bis(2-pyridylmethyl)ethylene-1,2-diamine].[3b,10]

Spectroscopic Characterization of Complexes 1−3

Solid-state (powder) Mössbauer spectroscopy (77 K) showed a doublet with comparable isomer shifts at about $\delta = 1.1$ mm·s^{-1} for each of the complexes, in accordance with a high spin state for the ferrous ions. Significantly different quadrupole splitting values ΔE_q were observed, however (Table 2).[11] The highest ΔE_q value was found for **3**, in agreement with the lower degree of symmetry resulting from two different monodentate ligands in the iron coordination sphere (see Table 2). It has to be noted that in the solid-state, the spin state of complex **2** differs from that in the crystal, revealing the importance of the packing in the crystal, and suggesting the involvement of a network of hydrogen bonds between the anions. This behavior is characteristic of related spin crossover systems.[12]

The complexes retained their structure in solution as they remained all monomeric in acetonitrile solution as indicated by their ESI/MS spectrum (Table 2). The UV/Visible spectra of acetonitrile solutions exhibit only one intense band in each case at around 400 nm, attributable to a MLCT band from Fe^{II} "t_{2g}" orbitals to π* orbitals of the pyridine ligands. Interestingly, it has been previously shown that the value of the extinction coefficient can be correlated with the ligand field strength.[13] The trend observed here, confirmed the order of the series found in the solid state.

Table 1. X-ray structural parameters (bond lengths and angles) for FeL(XY) complexes with X and Y = Cl and/or CH_3CN

Bond lengths (Å)	**1**	**3**	**2**
Fe−Cl	2.4260(2) 2.4080(2)	2.3383(3)	
Fe−$NCCH_3$		2.1730(8)	1.942(4) 1.945(4)
Fe−N_{amine}	2.3272(7) 2.3012(6)	2.2475(7) [N1] 2.2787(7)[N2]	2.056(3) 2.060(3)
Fe−$N_{pyridine}$	2.2120(2) 2.2228(6)	2.1708(8) 2.1717(8)	1.982(4) 1.990(4)
Angles (°)			
Cl−Fe−Cl	102.274(8)		
Cl−Fe−$N_{nitrile}$		96.6(2)	
$N_{nitrile}$−Fe−$N_{nitrile}$			91.50(15)
N_{amine}−Fe−N_{amine}	78.07(2)	80.50(2)	86.11(13)
$N_{pyridine}$−Fe−$N_{pyridine}$	169.67(2)	168.69(3)	178.39(15)
$N_{nitrile}$−Fe−$N_{pyridine}$		93.57(3)	94.85(16) 85.41(15)
N_{amine}−Fe−$N_{pyridine}$	75.17(8) 96.70(2)	75.77(3) 96.32(3)	81.04(15) 98.23(14)
$N_{nitrile}$−Fe−N_{amine}		174.94(19)	91.36(14) 175.17(14)
Cl−Fe−N_{amine}	90.40(2) 161.82(2)	95.43(18)	

The three complexes were also characterized by ^{1}H NMR spectroscopy at room temperature in CD_3CN solutions (Figure 2). The spectra show proton resonances between −20 and 140 ppm, a range typical for high spin ferrous (S = 2) complexes. A comparison of ^{1}H NMR spectra showed that the three complexes have different structures in solution. Proton assignments have been carried out from a comparison with related complexes, integrations, and T_1 values (see Table 3).[14] The pyridyl resonances are subject to large isotropic shifts in the following order α > β> γ based on the fact that the paramagnetic contact shifts are governed by σ-delocalization effects, so that the shifts increase with closer proximity to the ferrous ion.[15]

Thus, the α-pyridyl protons were assigned to the resonance at lower field, i.e. above δ = 130 ppm. Moreover, the β-pyridyl proton resonances, easily recognizable as they are usually assigned to two close sharp resonances at around δ = 50 ppm, shifted from 59/53 (β/β′) ppm for complex **1** to 52/44 and 48/40 ppm for complexes **3** and **2**, respectively.[14] Finally, the γ-H resonances were observed at δ = 21 ppm for **1**, and were found upfield for **2** and **3** at δ = 10 ppm and −8 ppm, respectively. The methylene CH_2 resonances can be assigned to the broader resonances spread throughout the spectra (see for example spectrum 2 in Figure 2). The number of these resonances signify the distinction between the two protons of the methylene moieties, a fact which is related to their position with regard to the metal ion. The methylene protons of CH_2−Pyr were tentatively attributed to the broad resonances in the 120−40 ppm region by comparison with the TPA complexes.[14] The methylene protons of the diamino and benzyl moieties of the ligand were less shifted, and were sensitive to the nature of the monodentate ligand set trans to the aliphatic amine.

We have tentatively attributed the upfield shift of the α,β,γ− pyridyl protons and the methylene protons in complex **2** to a lower paramagnetism compared with in **1** and **3**. It should be noted that the resonances of the protons of the trimethoxyphenyl moieties could not be assigned due to the presence of several overlapping peaks in the diamagnetic region of the spectra.

Remarkably, the spectra of **2** and **3** display broader resonances, suggesting ligand exchange in solution. This was confirmed when the NMR spectra were recorded in a non-coordinating solvent, i.e. CD_2Cl_2. Only the spectra of complexes **2** and **3** were different in terms of isomeric shifts and the broadness of the peaks. This is in agreement with the solvent ligand (CH_3CN) being more labile than the coordinated chloride. Conversely, this confirms that the chloride anions in complexes **1** and **3** remain iron-bound in acetonitrile solution, and that solutions of **3** do not contain a mixture of **1** and **2**.

Finally, Table 2 also shows that, as expected, the three complexes have different Fe^{III}/Fe^{II} potentials in acetonitrile. The cyclic voltammograms in CH_3CN/TBAP 0.1 M display one quasi-reversible process (ΔE = 100 mV) for **1** and **2**, whereas two systems of waves were observed on the reverse scan in the case of **3**. The presence of these two reduction peaks was attributed to an EC process, which has been assigned to the minor formation of $[FeLCl_2]^+$ (less than 10%) during the one-electron oxidation process of **3**. Accordingly, the location of the reducing wave of this minor electroactive

Table 2. Physical properties of FeL(XY) complexes with X and Y = Cl and/or CH_3CN

Complex	**1**	**3**	**2**
$\lambda_{max.}$ (ε [$M \cdot cm^{-1}$])	415 nm (1050)	373 nm (1350)	370 nm (1700)
E_{pa} [V/NHE]	0.560	1.12	1.43
E_{pc} [V/NHE]	0.430	0.930; 0.520[a]	1.33
δ [$mm \cdot s^{-1}$] [b]	1.14	1.12	1.15
δ [$mm \cdot s^{-1}$]	3.05	3.24	2.81
ESI/MS fragment	m/z = 693 ($[FeLCl]^+$)	m/z = 693 ($[FeLCl]^+$)	m/z = 757 ($[FeL(ClO_4)]^+$)

[a] Minor wave (less than 10% in intensity compared to the one at 0.930 V). [b] Referenced to α-Fe at 300 K.

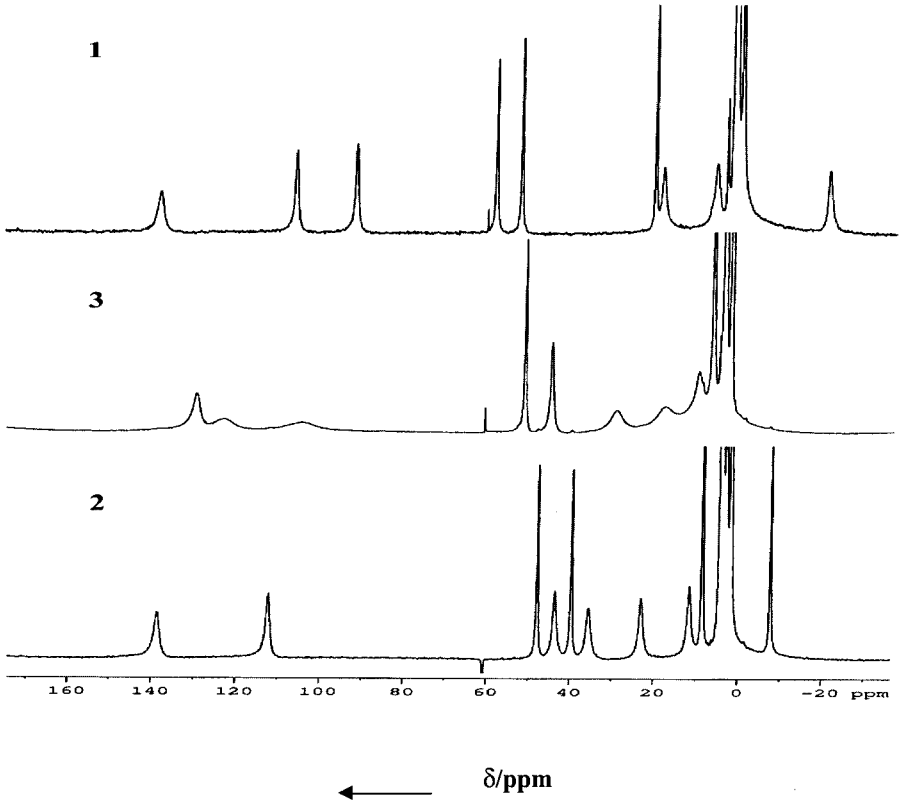

Figure 2. ^{1}H NMR spectra of complexes **1**−**3** in CD_3CN at room temperature

Table 3. ^{1}H NMR spectroscopic data for complexes **1**−**3**

Complex assignment	**1**	**3**	**2**
α-*H*pyr	140	131	138
β,β′-*H*pyr	59; 52	52; 44	48; 39.7
γ-*H*pyr	20.7	10(br)	−8
C*H*$_2$−Pyr	107; 92.7	123; 114	112;43.5
C*H*$_2$−Bz or	19; 6.5	18; 9	35.5; 23
C*H*$_2$-diamine	0.3; −21	4; 3	11.5; 3.2

species was observed close to that observed for **1**. As expected, the easier system to oxidize is **1**, followed by **3** then **2**. The presence of chloride anions in the coordination sphere implicates a decrease in oxidation potential of about 500 mV per anion.

To conclude, the three complexes have different structures in solution. We have thus obtained and fully characterized a series of complexes containing the same tetradentate ligand, and various combinations of chloride and acetonitrile ligands. These complexes can be used to study the effect of the nature of monodentate ligands and the number of labile sites on their ability to catalyze alkane oxidations. It should be noted that they retain their structures during redox processes. These results are presented in the next section.

Ligand Oxidation − A Probe for Hydroxyl Radical Generation

The reaction of complex **1** with hydrogen peroxide in the absence of an external substrate led to the formation of a new chromophore.[9] This chromophore has been characterized as a phenolato complex $[Fe^{III}LOCl]^+$, and resulted from hydroxylation, at the *ortho* position, of one phenyl moiety of the ligand L (Scheme 2). No such species could be observed during reaction of complex **2** with H_2O_2 under the same conditions. On the other hand, in the presence of 10 equivalents of H_2O_2 in acetonitrile, complex **3** was partly converted into this chromophore as shown by ESI-MS with a molecular ion peak at m/z = 708. When $H_2{}^{18}O_2$ was used, only one peak at m/z = 710, corresponding to the $[Fe^{III}(L^{18}O)Cl]^+$ fragment, was present. This signifies that the inserted oxygen came exclusively from the oxidant.

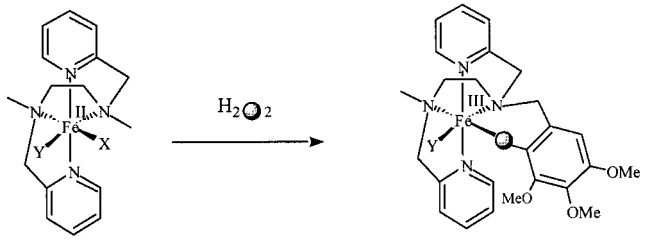

Scheme 2. Chemical transformation of ferrous complexes **1** and **3** using hydrogen peroxide

However, the yield of ligand hydroxylation was found to be much lower than in the case of **1**. Ligand extraction from the mother liquor confirmed the ligand oxidation, and quantitative analysis showed that the oxidized ligand LOH was preferentially formed with complex **1** (yield = 60%), in contrast to the result with complex **3** (15%) (see Table 4). With all complexes, minor formation of ligand L1, *N*,*N*′-bis(pyridin-2-ylmethyl)-*N*-(3,4,5-trimethoxybenzyl)ethane-1,2-diamine, was detected (<15%).[9] L1 results from an *N*-dealkylation of the ligand L following hydroxylation at one of the benzylic positions.

Table 4. Comparison of the oxidizing properties of complex **1**, **2**, and **3** (experimental conditions: CH_3CN, room temp., Ar; [complex] = 1 mM; [complex]/substrate/H_2O_2, 1:100:10

Complex	**1**	**3**	**2**
Ligand L oxidation[a]			
L (%)	6	60	60
L−OH (%)	70	15	0
L1 (%)	7	14	14
Cyclohexane			
cyclohexanol (% yield[b])	3	7	23
cyclohexanone	1	3	2.5
ol/one [c]	3	2	9.2
cis-DMC			
cis-OH (%[b])	4	7	20
trans-OH	2.5	3	3
% RC[d]	20	40	74
Cyclooctene			
epoxide (%[b])	0	6	31
Cyclohexene			
epoxide (%[b])	0	7	5
2-cyclohexene-1-ol	2	24	9
2-cyclohexene-1-one	0	6	1

[a] Only the three major products analyzed by HPLC have been reported. [b] Yield based on the oxidant. [c] ol/one corresponds to the ratio of cyclohexanol over cyclohexanone. [d] % RC = 100 × (*cis*-OH-*trans*-OH)/(*cis*-OH + *trans*-OH) with an error estimated to be ± 5%; *cis*-OH = (1*R*,2*R*- or 1*S*,2*S*)-1,2-dimethylcyclohexanol. *trans*-OH = (1*R*,2*S*- or 1*S*,2*R*)-1,2-dimethylcyclohexanol.

OH radicals are excellent agents for aromatic hydroxylation.[6] Thus the formation of LOH from the oxidation of L by H_2O_2 was used here as a probe for the presence of $OH^{\cdot}$ radicals derived from H_2O_2. Our results thus show a dramatic difference between **2**, on the one hand, and **1** and **3**, on the other hand, in terms of generation of $OH^{\cdot}$ radicals. Only complex **2** was unable to convert H_2O_2 into $OH^{\cdot}$. It is also important to note that in the case of **3**, LOH is a minor product whereas in the case of **1**, L is extensively converted into LOH, indicating a more significant involvement of $OH^{\cdot}$ radicals in reactions catalyzed by **1**. This is supported by the observations reported below.

Hydrocarbon Oxidation

In a typical reaction, 2 μmol of complex $[FeLXY](ClO_4)_n$ [n = 0 for complex **1**, 1 for **3** and 2 for **2**] in acetonitrile (final volume = 2 mL) was treated with 20 μmol of H_2O_2 (10 equiv.) in the presence of 1100 equiv. of the alkane in acetonitrile at room temperature under argon. All the reactions were complete after 10 minutes by which time the oxidant was completely consumed. No oxidation occurred in the absence of the iron complex. Complex **2** was found to be the most active catalyst during oxidation of cyclohexane with a 30% total yield based on the oxidant, followed by complex **3** (13%), and **1** (4%). The same pattern was observed when the selectivity of the hydroxylation was considered with an alcohol/ketone ratio above 9 for complex **2** (Table 4), whereas much less selectivity was observed with complexes **3** and **1**.

Furthermore, only complex **2** could catalyze stereoselective hydroxylations (Table 4). For example, oxidation of *cis*-1,2-dimethylcyclohexane gave *cis*-1,2-dimethylcyclohexanol (1*R*,2*R* or 1*S*,2*S*) as the major product (%RC over 70%) showing that hydroxylation proceeds preferentially with retention of configuration at C-1, thus excluding a pure radical mechanism. Much less stereoselectivity was observed with complexes **3** and **1** (%RC = 40% and 20%, respectively).

Ligand hydroxylation and alkane oxidation reactions clearly make it possible, therefore, to distinguish **2** from **1** and **3**, but not **1** from **3**. In contrast, alkene epoxidation, as discussed below, provides a convenient reaction probe to make this distinction. Indeed, whereas epoxides are formed during oxidation of cyclohexene and cyclooctene by H_2O_2 in the presence of **2** and **3**, no epoxide could be detected with complex **1** as the catalyst. In the latter case, only very little allylic alcohol could be detected with cyclohexene as the substrate. Here, epoxidation is used as a probe for the involvement of metal-oxo intermediate active species.[16] Thus, these results suggest the presence of such species in reactions catalyzed by **2** or **3**, but not in reactions catalyzed by **1**. The involvement of a $[Fe{=}O]^{n+}$ species is further supported by the observation of ^{18}O labeled cyclohexanol during cyclohexane oxidation by H_2O_2 in the presence of 1000 equivalents of $H_2{}^{18}O$ (complex **2**: 47%, complex **3**: 5%). This is due to the ability of (per)ferryl complexes to exchange O atoms with H_2O.[17] The presence of products labeled with O atoms from both water and the oxidant has already been observed in oxidations dependent on non-heme iron complexes.[18]

Evidence for Iron-Hydroperoxo Complexes During the Reaction

Iron hydroperoxo complexes have been extensively studied during the last decade.[1,19,20] They are usually characterized by a LMCT band in the visible region, from which a resonance Raman spectrum dominated by O−O and Fe−O vibrations may be observed.[21] Using a previously described methodology,[22] which consists of low temperature mixing of the oxidant and the catalyst, we were able to detect such an Fe−OOH species by ESI-MS in some cases. Firstly, fast mixing of complex **3** with 10 equivalents of H_2O_2 resulted in the detection of a new peak at m/z = 726, which we assigned to the $[FeLOOHCl]^+$ fragment, with excellent agreement between its observed and theoretical isotopic patterns (see Supporting Information S1). The assign-

ment was confirmed, during an MS/MS experiment, by the loss of a fragment of $m/z = 33$ corresponding to the OOH fragment. A corresponding shift of +4 in the parent peak was observed when $H_2{}^{18}O_2$ was used. In contrast, with complex **1**, no Fe−OO(H) could be detected, whereas with complex **2** different fragments were observed at $m/z = 790$ and 345.5. These were assigned to $[FeLOOHClO_4]^+$ and $[FeLOOH]^{2+}$, respectively (Supporting Information S2). The fact that this fragment was absent in the mass spectrum of **3**/H_2O_2 indicates that complex **2** was not a contaminant in solutions of complex **3**.

The presence of a hydroperoxo ferric complex $[X-Fe^{III}-OOH]^{n+}$ in the case of **2** and **3** but not **1**, strongly suggests a distinct reaction pathways in systems dependent on **1** and **3**.

Discussion

Using a variety of reaction probes we have clearly demonstrated that the three complexes under study have very different catalytic properties during oxidation by hydrogen peroxide, even though they contain the same tetradentate nitrogen-based ligand L.

In the case of complex **1**, the extensive conversion of L to LOH by aromatic hydroxylation, the low alcohol/ketone ratio, the low stereoselectivity during alkane oxidation, and the lack of epoxide formation during alkene oxidation suggest that freely diffusing hydroxyl radicals are the active species.[23]

In contrast, in the case of complex **2**, the lack of LOH formation, the high alcohol/ketone ratio, the large stereoselectivity, the fact that oxygens from exogenous water molecules are incorporated into the products, and its ability to epoxidize alkenes are in agreement with a selective metal-based mechanism.

Complex **3** displays some of the properties of complex **1** (formation of LOH, low stereoselectivity), and some of those of complex **2** (epoxidation, formation of an Fe-hydroperoxo complex, and cyclohexanol labeling with $H_2{}^{18}O$). This, then, suggests a third type of mechanism involving both [Fe=O] and OH radical species.

What differentiates complexes **1**−**3** from each other is the number of labile coordination sites. We have shown that in solution, Cl^- ligands are not exchangeable with the solvent even when the iron center is in the ferrous state. In contrast CH_3CN ligands are exchangeable. As a consequence, complex **1** has no exchangeable ligand, complex **3** has one, and complex **2** has two. We thus propose that the number of labile coordination sites defines the type of reaction mechanism, namely the type of active species responsible for substrate activation and oxygen atom insertion (Scheme 3).

In the case of complex **1**, H_2O_2 cannot bind to iron, in agreement with the fact that no Fe−OOH species could be detected. This iron reacts with H_2O_2 via an outer sphere one-electron redox process generating OH radicals with good aromatic hydroxylation and poor epoxidation power. In the case of complex **2**, H_2O_2 can bind to iron to form an intermediate Fe−OOH complex, as shown by ESI-MS. It is proposed that the latter proceeds by heterolytic O−O cleavage to generate an active $[Fe^V=O]$ species, allowing a more selective metal-based oxo transfer process.

In the case of complex **3**, with a single exchangeable coordination site, H_2O_2 can also bind to iron. Indeed an Fe−OOH complex has also been detected in this case by ESI-MS. It can be proposed, however, that the latter proceeds by homolytic (and not heterolytic) cleavage of the O−O bond thus generating both $[Fe^{IV}=O]$ and $OH^{\cdot}$ species, in agreement with the properties of the oxidation reaction catalyzed by **3**.

The question thus arises, whether the rather drastic difference between **2** and **3** results only from the difference in terms of labile sites or for an additional reason. Studies by L. Que Jr. and co-workers have shown the importance of the presence of two labile sites for promoting heterolytic cleavage.[18] In particular, the possibility for the terminal oxygen of the Fe−OOH species to interact with iron via binding to the second site provides a major driving force for the heterolytic cleavage of the O−O bond. A second possibility comes from the binding of a molecule of H_2O to the second site, which can thus promote O−O heterolytic cleavage by donating a proton.

In the case of complex **3**, a Cl−Fe−OOH species is formed, and there is no such driving force for heterolytic cleavage because of the presence of a non-exchangeable Cl ligand. As a consequence, only a homolytic cleavage takes place. We have thus shown here, from a detailed comparison of **2** and **3**, that the number of labile sites has a great impact on the outcome of the oxidation reactions involving Fe−OOH intermediates. Previous studies by Que Jr. and Feringa and co-workers have raised a similar issue. They did it on the basis of the comparison of $[Fe(TPA)(CH_3CN)_2]^{2+}$ complexes with diverse ligand sub-

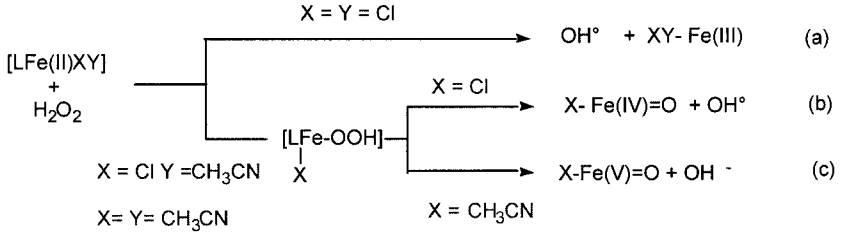

Scheme 3. The three reaction pathways for iron/H_2O_2 systems as a function of the ligands X and Y

stitutions − which are catalysts of oxidation reactions proceeding by metal-based mechanisms −, with the $[Fe(N4py)(CH_3CN)]^{2+}$ complex, in which N4py is a pentadentate ligand related to TPA (Scheme 1).[18,24] The latter has only one exchangeable site, and is not able to catalyze the epoxidation of alkenes by H_2O_2.

On the other hand, it should be recalled that in the case of reactions of Fe-porphyrins with *m*-chloroperbenzoic acid (*m*CPBA), cleavage of the O−O bond within the intermediate Fe−OOC(O)R complex is dependent on the nature of the axial ligand trans to the acylperoxo ligand.[25] The cleavage is homolytic when this ligand is Cl^-, and heterolytic with less electron donating anions such as ClO_4^-. In the case of **2** and **3**, we might also consider that, rather than the exchangeability of the sites, it is the electronic properties of the ligands (Cl^- vs. CH_3CN) which influence the cleavage of the O−O bond of the X−Fe−OOH species. Further experiments are needed to better establish the importance of such electronic effects in these catalysts.

Conclusion

The structural parameters required for efficient iron catalysts for selective oxidations using hydrogen peroxide as the oxidant have been elucidated. The presence of neutral nitrogen ligands (allowing a high Lewis acidity for the metal for H_2O_2 activation), and the presence of two labile sites (to favor the heterolytic cleavage of the O−O bond) are required for selective and efficient catalysis of alkane hydroxylation. The control of the O−O bond cleavage by anions needs to be better understood, and the charge on the X ligand is probably an important parameter to consider. So far, complex **2** represents one of the more efficient catalyst in its category.

Experimental Section

General: Most of the reagents were of the best commercial grade, and were used without further purification. The synthesis of ligand L has been described previously.[8]

Synthesis of Complex 1: In a glove box, $FeCl_2{\cdot}4H_2O$ (150 μmol) was added to a methanolic solution (8 mL) of ligand L (150 μmol). The solution rapidly turned yellow, and was stirred for two hours under an inert atmosphere at room temperature. The resultant powder was filtered, and washed with diethyl ether. Crystals suitable for X-ray crystallography were obtained by diffusion of diethyl ether into an acetonitrile solution of complex **1**. The powder was found to be stable under aerobic conditions.

Synthesis of Complex 2: In a glove box, $Fe(ClO4)_2{\cdot}4H_2O$ (150 μmol) was added to a methanolic solution (8 mL) of ligand L (150 μmol). The solution was stirred until complete precipitation of a pale yellow powder. After filtration, the powder was washed twice with diethyl ether. Purple crystals of complex **2** were obtained from diffusion of diethyl ether into an acetonitrile solution but the crystals were unsuitable for X-ray crystallography. X-ray quality crystals for **2** were obtained after a metathesis of ClO_4 for PF_6 anions. The powder was found to be less stable in air than complex **1**.

Synthesis of Complex 3: Complex **2** (32 mg, 36 μmol) was added to a $CHCl_3$ or CH_2Cl_2 solution of complex **1** (27 mg, 36 μmol) under an Ar atmosphere, and stirred for 1 h. A light yellow powder progressively appeared (yield >90%). The solid was washed with diethyl ether, and analyzed by ESI-MS and ^{1}H NMR spectroscopy. The spectroscopic data are consistent with the description of the complex as a dinuclear compound $[Fe_2L_2Cl_2(ClO_4)_2]$. The presence of two chloro bridges led, in this case, to a small ferromagnetic coupling as indicated by a CH_2Cl_2 X-band EPR (parallel mode) signal (g = 16, T = 4 K). This is a characteristic signature for an integral spin ground state (data not shown).[26] This was also corroborated by the larger range for the proton resonances observed by ^{1}H NMR spectroscopy in the dinuclear complex, compared with those in complexes **1** and **2** (for example, the α-H resonance of the bound pyridine moieties was observed at δ = 180 ppm, whereas it was found at around δ = 140 ppm in **1** and **2**). Solid-state Mössbauer parameters are in agreement with the high-spin configuration of the two identical ferrous atoms of the dinuclear unit (δ = 1.10 mm·s^{-1} and δ = 1.28 mm·s^{-1}). ESI-MS: m/z = 1485 (50%), $[Fe_2L_2Cl_2ClO_4]^+$: m/z = 1421 (100%) $[Fe_2L_2Cl_3]^+$. ^{1}H NMR (CD_2Cl_2): δ = 180.2 (α-H py); 49.0, 46.5 (β-H py). 155.1, 50.3 (CH_2-py). 31.0, 24.7(CH_2−Et). 70.0, 51.0 [(CH_2−Bz), 10.2 (Ar−O−*Me*), 11.4 (*p*-*H*-Benzyl), −7.2 (γ-*H*-py) ppm.
To obtain complex **3**, the yellow powder was dissolved in acetonitrile, and crystals were grown by diffusion of ether into this acetonitrile solution.

Crystallographic Studies: Data collection and analyses of complexes **1**-**3** were conducted on a Bruker SMART CCD system at the crystallography service of the SCIB laboratory (CEA-Grenoble). Experimental conditions for complex **3**: **3**·0.5$(C_2H_5)_2O$·0.5H_2O ($C_{38}H_{51}Cl_2FeN_5O_{11}$): M = 880.59 g mol^{-1}, yellow plate, triclinic, collection temperature 223 K, space group $P\bar{1}$, a = 10.9451(7) Å, b = 13.3551(8) Å, c = 15.746 (1) Å, α = 94.719 (1)°, β = 105.831(1)°, γ = 97.859(1)°, V = 2176.5(2) Å^3, Z = 2, $R1$ = 0.0515 [I = 2σ(I)]. Pertinent crystallographic data are reported in Table 1, full data can be obtained from the Cambridge Crystallographic Data Centre. The structures were solved by direct methods using the SHELXTL 5.03 software package. All non-hydrogen atoms were refined anisotropically. Hydrogen atoms were placed in ideal positions, and refined as riding atoms with individual (or group) isotropic displacements. CCDC-146454, -146455, and -226070 contain the supplementary crystallographic data for **1**, **2**, and **3**, respectively. These data can be obtained free of charge at www.ccdc.cam.ac.uk/conts/retrieving.html [or from the Cambridge Crystallographic Data Centre, 12 Union Road, Cambridge CB2 1EZ, UK; Fax: (internat.) +44-1223-336-033; E-mail: deposit@ccdc.cam.ac.uk].

Physical Studies: 300-MHz ^{1}H-NMR spectra were recorded on a DPX300 Bruker spectrometer, and the shifts referred to the residual solvent peak. Visible absorption spectra were recorded on Varian Cary1Bio and HP 8453 diode array spectrophotometers. Gas chromatography (GC) was performed on a Perkin−Elmer Autosystem instrument with a FID detector, using an SE 30 column coupled to a Perkin−Elmer Turbomass EI spectrometer. Mössbauer spectra were recorded in 400 μL cups containing the complex as a solid with a conventional constant acceleration spectrometer using a ^{57}Co source in a Rh matrix (1.85 Gbq). ESI-MS spectra were obtained on an LCQ ion trap spectrometer. Cyclic voltammetry experiments were performed using a PAR model 273 potentiostat/galvanostat. The working electrode was a platinum disc.

Ligand Extraction and Titration of the Products After Oxidation Reactions: After the completion of the reaction between the com-

plex and hydrogen peroxide followed by UV/visible spectroscopy the solvent was removed, and water was added until a concentration of 5 mM, based on starting iron concentration, was reached. Excess dithionite was then added, and 5 equivalents of bathophenanthroline were added. The total complexation of iron by the dinitrogen ligand was followed by UV/Visible spectroscopy (ε_{535nm} = 22140 $M^{-1}\cdot cm^{-1}$) and, when complete, the organic products were extracted with dichloromethane. The products were analyzed by ^1H and ^{13}C NMR spectroscopy and ESI-MS. Quantitative analysis of the components of the mixture was performed using HPLC based on the titration curves of pure samples. The total content never reached 100% due to the presence of minor products observed on the HPLC chromatogram.

Oxidation Reactions: In a typical reaction, 10 equivalents of H_2O_2 were added to a 1 mM solution of complex containing 1100 equivalents of cyclohexane (or 600 equiv. of 1,2-dimethylcyclohexane) or alcene in a glove box. The reaction was complete after 15 minutes, and the oxidation products were analyzed by GC/MS chromatography using benzophenone or acetophenone as an internal standard. The products were identified by ESI-MS, and titration curves were performed using pure samples to enable a quantitative analysis of the products.

Supporting Information: ESI/MS spectrum of **2**/H_2O_2 (S1) and ESI/MS spectrum of **3**/H_2O_2 (S2).

Acknowledgments

We thank the Iron-oxygen protein network (ERBFMRXCT980207) of the T. M. R. program of the E.U.

[1] [1a] E. I. Solomon, T. C. Brunold, M. I. Davis, J. N. Kemsley, S.-K. Lee, N. Lehnert, F. Neese, A. J. Skulan, Y.-S. Yang, J. Zhou, *Chem. Rev.* **2000**, *100*, 235. [1b] L. Que Jr., R. Y. N. Ho, *Chem. Rev.* **1996**, *96*, 2607.

[2] [2a] M. Fontecave, S. Ménage, C. Duboc-Toia, *Coord. Chem. Rev.* **1998**, *178*, 1555. [2b] M. Costas, L. Que Jr., *Coord. Chem. Rev.* **2000**, *200*, 517.

[3] [3a] C. Kim, K. Chen, L. Que Jr., *J. Am. Chem. Soc.* **1997**, *119*, 5964. [3b] K. Chen, L. Que Jr., *Chem. Commun.* **1999**, 1375.

[4] I. Schlichting, J. Brerenzen, K. Chu, A. M. Stock, S. A. Maves, D. E. Benson, R. M. Sweet, D. Ringe, G. A. Petsko, S. G. Sligar, *Science* **2000**, *287*, 1615.

[5] J.-U. Rohde, J.-H. In, M. H. Lim, W. W. Brennessel, M. K. Bukowski, A. Stubna, E. Münck, W. Nam, L. Que Jr., *Science* **2003**, *299*, 1037.

[6] [6a] C. Walling, *Acc. Chem. Res.* **1975**, *8*, 125. [6b] P. A. Mc Faul, D. D. M. Wayner, K. U. Ingold, *Acc. Chem. Res.* **1998**, *31*, 159. [6c] D. T. Sawyer, A. Sobkowiak, T. Matsushita, *Acc. Chem. Res.* **1996**, *29*, 409.

[7] S. Ménage, J.-M. Vincent, C. Lambeaux, G. Chottard, A. Grand, M. Fontecave, *Inorg. Chem.* **1993**, *32*, 4766.

[8] S. Ménage, J. B. Galey, J. Dumats, G. Hussler, M. Seité, I. Gautier-Luneau, G. Chottard, M. Fontecave, *J. Am. Chem. Soc.* **1998**, *120*, 1337.

[9] Y. Mekmouche, S. Ménage, C. Toia-Duboc, M. Fontecave, J.-B Galey, C. Lebrun, J. Pécaut, *Angew. Chem. Int. Ed.* **2001**, *40*, 949.

[10] J. Simaan, S. Poussereau, G. Blondin, J.-J. Girerd, D. Defaye, C. Philouze, J. Guilhem, L. Tchertanov, *Inorg. Chim. Acta* **2000**, *299*, 221.

[11] A. X. Trautwein, E. Bill, E. L. Bominaar, H. Winkler, *Struct. Bonding* **1991**, *78*, 1.

[12] H. R. Chang, J. K. McCuster, H. Toftlund, S. R. Wilson, A. X. Trautwein, H. Winkler, D. N. Hendrickson, *J. Am. Chem. Soc.* **1990**, *112*, 6814.

[13] [13a] P. Mialane, A. Nivorojkine, G. Pratviel, L. Azéma, M. Slany, F. Godde, A. Simaan, F. Banse, T. Kargar-Grisel, G. Bouchoux, J. Sainton, O. Horner, J. Guilhem, L. Tchertanova, B. Meunier, J.-J. Girerd, *Inorg. Chem.* **1999**, *38*, 1085. [13b] H. R. Al-Obaidi, K. B. Jensen, J. J. McGarvey, H. Toftlund, B. Jensen, S. E. J. Bell, J. G. Carroll, *Inorg. Chem.* **1996**, *35*, 5055.

[14] Y. Zang, J. Kim, Y. Dong, E. C. Wilkinson, E. H. Appelman, L. Que Jr., *J. Am. Chem. Soc.* **1997**, *119*, 4197.

[15] L.-J. Ming in *Physical Methods in Bioinorganic Chemistry* (Ed. L. Que Jr.), University Science Book, Sausalito, CA, **2000**, chapter 8.

[16] [16a] M. Sono, M. P. Roach, E. D. Coulter, J. H. Dawson, *Chem. Rev.* **1996**, *96*, 2841. [16b] W. Nam, S.-E. Park, I. K. Lim, M. H. Lim, J. Hong, J. Kim, *J. Am. Chem. Soc.* **2003**, *125*, 14674 and references cited therein.

[17] J. Bernadou, B. Meunier, *Chem. Commun.* **1998**, 2167.

[18] K. Chen, L. Que Jr, *J. Am. Chem. Soc.* **2001**, *121*, 6327.

[19] J.-J. Girerd, F. Banse, A. J. Simaan, *Struct. Bonding* **2000**, *97*, 143.

[20] G. Roelfes, V. Vrajmasu, K. Chen, R. Y. N. Ho, J.-U. Rohde, C. Zondervan, R. M. la Crois, E. P. Schudde, M. Lutz, A. L. Spek, R. Hage, B. L. Feringa, E. Münck, L. Que Jr., *Inorg. Chem.* **2003**, *42*, 2639.

[21] [21a] Y. Mekmouche, H. Hummel, R. Y. N. Ho, L. Que Jr., V. Schüenemann, F. Thomas, A. X. Trautwein, C. Lebrun, K. Gorgy, J. C. Leprêtre, M.-N. Collomb, A. Deronzier, M. Fontecave, S. Ménage, *Chem. Eur. J.* **2002**, *8*, 1196. [21b] R. Y. N. Ho, G. Roelfes, B. L. Feringa, L. Que Jr., *J. Am. Chem. Soc.* **1999**, *121*, 264.

[22] J. Kim, Y. Dong, E. Larka, L. Que Jr., *Inorg. Chem.* **1996**, *35*, 2369.

[23] [23a] A. F. Trotman-Dickenson, *Adv. Free Radical Chem.* **1965**, *1*, 1. [23b] G. V. Buxton, C; L. Greenstock, W. P. Helman, A. B. Ross, *J. Phys. Chem. ref. Data* **1988**, *17*, 513. [23c] S. Miyajima, O. Simamura, *Bull. Chem. Soc. Jpn.* **1975**, *48*, 526.

[24] G. Roelfes, M. Lubben, R. Hage, L. Que Jr., B. L. Feringa, *Chem. Eur. J.* **2000**, *6*, 2152.

[25] [25a] W. Nam, M. H. Lim, S.-Y. Oh, J. H. Lee, H. J. Lee, S. K. Woo, C. Kim, W. Shin, *Angew. Chem. Int. Ed.* **2000**, *39*, 2179. [25b] W. Nam, M. H. Lim, S. K. Moon, C. Kim, *J. Am. Chem. Soc.* **2000**, *122*, 10805.

[26] M. P. Hendrich, P. G. Debrunner, *Biophys. J.* **1989**, *56*, 489.

Received December 11, 2003
Early View Article
Published Online June 1, 2004

